23rd International Conference on Renewable Energies and Power Quality (ICREPQ'25)
Tenerife (Spain), 25th to 27th June 2025
Renewable Energy and Power Quality Journal (RE&PQJ)
ISSN 2172-038 X, Volume No.23, September 2025

Modeling of DC asymmetrical faults in bipolar HVDC links with metallic return

C. Wijnakker[1], J.L. Rodríguez-Amenedo[1], F. Arredondo[1] and S. Arnaltes[1]

[1] Departamento de Ingeniería Eléctrica
EPS, Universidad Carlos III de Madrid
Campus de Leganés – Av. de la Universidad, 30, 28911 Leganés, Madrid

Abstract. This work proposes a compact and flexible dynamic model of a bipolar HVDC link with metallic return, suitable for simulation of power systems. The model is formulated compactly using only two matrix equations and is capable of simulating different types of faults, including pole-to-ground, pole-to-neutral and pole-to-pole faults. The inclusion of the dynamic equations of the neutral cable enables accurate asymmetric perturbation dynamic studies. The proposed model has been included as a module in a software framework which is aimed for dynamic simulation studies in AC/DC systems. Results demonstrate the model's functionality and capability to simulate various fault types, including asymmetric faults, where the neutral cable plays a pivotal role.

Key words. HVDC transmission, metallic return, AC/DC power systems, fault modelling, time-domain simulation.

1. Introduction

High Voltage Direct Current (HVDC) has become increasingly important because its advantages mitigate the challenges that arise with the energy transition [1]. HVDC grids are not influenced by capacitance and inductance in a permanent regime, making them ideal for marine and subterranean lines which have high capacitance [2]. This is because in AC lines, high capacitance results in increased losses and complicates voltage control. The primary use of HVDC technology in the last decades has been the connection of offshore wind parks to the mainland, widely used in the North Sea, and the connection of islands to the mainland to strengthen their local grids and allow higher penetration of renewable energy. Additionally, HVDC excels in transmitting large amounts of power over long distances because it has no reactive power associated losses, making it ideal for transmitting power between remote regions and different climate areas [3], [4]. Another application of HVDC grids is the asynchronous connection of AC grids. In the coming years, the use of HVDC technology is expected to increase with various projects in construction and plans for multiterminal grids [5], [6].

Line Commutated Converters (LCCs) and Voltage Source Converters (VSCs) are the two primary technologies used in HVDC transmission. LCCs, while simpler and often less expensive, have limitations in control and depend on the AC system strength. VSCs, employing Insulated Gate Bipolar Transistors (IGBTs), offer greater flexibility and control [7]. However, the limitations of IGBTs have led to the development of Modular Multilevel Converters (MMCs) for higher power applications.

HVDC links employ various control strategies to manage power flow and maintain system stability. Common control modes include constant voltage control, constant power control, and droop control [8]. In a point-to-point HVDC link, typically one converter is operated in constant voltage control mode to establish a stable DC voltage level, while the other converter operates in constant power control mode to regulate the power flow across the link. This centralized control approach ensures reliable and efficient power transmission.

Most HVDC links are bipolar, employing two conductors to transmit power. While some HVDC systems utilize earth return, where the ground or sea acts as the return path for the current, metallic return is the most employed [9]. In simulations of asymmetrical faults in HVDC systems, accurate modeling of the metallic return path is crucial. This is because significant voltages and currents can develop in the return conductor, especially when the grounding point is located at a considerable electrical distance from the fault location [10]. In RMS studies of AC systems, grid modeling is typically algebraic, however, preserving the dynamics is convenient for HVDC systems [11]. Reference [12] shows that the line inductance affects significantly the short-circuit current, especially during the initial milliseconds following a fault.

The aim of this paper is to develop a compact and versatile model of a bipolar HVDC link with metallic return that enables the study of various types of contingencies (pole-to-pole, pole-to-ground and pole-to-neutral), line clearances and converter outages, with capability to simulate the asymmetries.

The contributions of this work are as follows: 1) The formulation of a compact and flexible model, using two matrix equations, of a point-to-point bipolar HVDC system with metallic return. The model allows for the straightforward accommodation and simulation of different types of faults in these systems; 2) A simulation software

framework in Matlab/Simulink using the proposed model, enabling simulations and analysis of HVDC systems under different fault scenarios in an easy manner.

A bipolar link with metallic return, connecting two AC systems through VSC converters, is modeled using the proposed framework. The VSC model is built based on Type 4 converter model from ESIG [13]. This paper presents results on how different types of faults affect operation and control in these systems.

2. HVDC bipolar link with metallic return

This section focuses on the development of the HVDC link with metallic return model, culminating in the derivation of the proposed dynamic equations in matrix form.

A. HVDC bipolar link with metallic return model

Fig. 1 shows the electric schematic of the HVDC link with bipolar return, where lines are represented by a π-model. The system connects two asynchronous AC grids, each consisting of three nodes, two lines and, a conventional synchronous generator, with one grid also including a load. The AC and DC grids are interconnected through 4 AC/DC converters.

Solving the node voltages for the HVDC grid model, five dynamic equations can be obtained:

$$\tau^{CAB}\frac{du^{A+}}{dt} = -i^{A+} - i^{+} \quad (1)$$

$$\tau^{CAB}\frac{du^{B+}}{dt} = -i^{B+} + i^{+} \quad (2)$$

$$\tau^{CAB}\frac{du^{A-}}{dt} = i^{A-} - i^{-} \quad (3)$$

$$\tau^{CAB}\frac{du^{B-}}{dt} = i^{B-} + i^{-} \quad (4)$$

$$\tau^{Co}\frac{du^{Bo}}{dt} = i^{B+} - i^{B-} + i^{o} \quad (5)$$

Where:

$i^{A+}, i^{B+}, i^{A-}, i^{B-}$ are the converter currents [p.u.],

$u^{A+}, u^{B+}, u^{A-}, u^{B-}, u^{Bo}$ are the node voltages [p.u.],

i^{+}, i^{-}, i^{o} are the line currents [p.u.], and

τ^{CAB}, τ^{Co} are the time constants of the capacitors [s] calculated with equation (6).

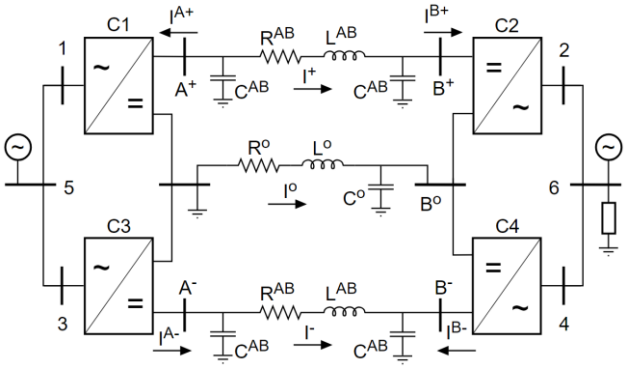

Fig. 1. Bipolar HVDC link model with metallic return.

$$\tau^{CAB} = \mathrm{Z}_b \cdot C^{AB} \quad (6)$$

Where:

Z_b is the base impedance [Ω], and

C^{AB} is the line capacitance [F].

The five dynamic equations can be expressed as the matrix equation (7), to make a compact model which simplifies its implementation in tools such as Matlab/Simulink:

$$\tau^{C}\frac{d[U]}{dt} = A[I^{L}] + B[I^{C}] \quad (7)$$

Where:

$[U] = [u^{A+}, u^{B+}, u^{A-}, u^{B-}, u^{Bo}]$ is the node voltages vector,

$[I^{L}] = [i^{+}, i^{-}, i^{o}]$ is the line currents vector,

$[I^{C}] = [i^{A+}, i^{B+}, i^{A-}, i^{B-}]$ is the converter currents vector,

$\tau^{C} = diag(\tau^{CAB}, \tau^{CAB}, \tau^{CAB}, \tau^{CAB}, \tau^{Co})$ is the converters time constants matrix,

$$A = \begin{bmatrix} -1 & 0 & 0 \\ 1 & 0 & 0 \\ 0 & -1 & 0 \\ 0 & 1 & 0 \\ 0 & 0 & 1 \end{bmatrix} \text{ and } B = \begin{bmatrix} -1 & 0 & 0 & 0 \\ 0 & -1 & 0 & 0 \\ 0 & 0 & 1 & 0 \\ 0 & 0 & 0 & 1 \\ 0 & 1 & 0 & -1 \end{bmatrix}.$$

Solving the currents for the HVDC grid model, another three dynamic equations can be obtained:

$$\tau^{LAB}\frac{di^{+}}{dt} = u^{A+} - u^{B+} - R^{AB} \cdot i^{+} \quad (8)$$

$$\tau^{LAB}\frac{di^{-}}{dt} = u^{A-} - u^{B-} - R^{AB} \cdot i^{-} \quad (9)$$

$$\tau^{Lo}\frac{di^{o}}{dt} = -u^{Bo} - R^{o} \cdot i^{o} \quad (10)$$

Where:

R^{AB}, R^{o} are the line resistances [p.u.], and

τ^{LAB}, τ^{Lo} are the time constants of the line inductances [s], calculated following equation (11).

$$\tau^{LAB} = \frac{L^{AB}}{\mathrm{Z}_b} \quad (11)$$

Where:

L^{AB}, L^{0} are the line inductances [H].

The three dynamic equations can be compacted and expressed as matrix equation (12):

$$\tau^{L}\frac{d[I^{L}]}{dt} = C[U] + D[I^{L}] \quad (12)$$

Where:

$\tau^{L} = diag(\tau^{LAB}, \tau^{LAB}, \tau^{Lo})$ is the line inductances time constants matrix,

$C = -A^{T}$ and

$D = diag(-R^{AB}, -R^{AB}, -R^{o})$.

In conclusion, the bipolar HVDC link with metallic return dynamic model is described with matrix the equations (7)

and (12). In the dynamic model $[U]$ and $[I^L]$ are the state variables and $[I^C]$ the input variables.

B. Fault modelling

The proposed model enables the analysis of eight different types of contingencies that consist in pole-to-ground, pole-to-pole and pole-to-neutral faults. Table I summarize all of them.

Table I. – Fault types

Name	Type	From	To
A+	Pole-to-ground	A+	Ground
B+	Pole-to-ground	B+	Ground
A-	Pole-to-ground	A-	Ground
B-	Pole-to-ground	B-	Ground
AA	Pole-to-pole	A+	A-
BB	Pole-to-pole	B+	B-
Bo+	Pole-to-neutral	B+	Bo
Bo-	Pole-to-neutral	Bo	B-

In this work, the fault impedance is modelled as a resistance. The fault current in the HVDC model is calculated using the following equation:

$$i^{SC} = G^{SC} \cdot (u^{FROM} - u^{TO}) \tag{13}$$

Where:

i^{SC} is the short-circuit current [p.u.],

G^{SC} is the short-circuit conductance [p.u.],

u^{FROM} is the voltage at the node where the short-circuit occurs [p.u.], and

u^{TO} is the voltage at the second node, where the short-circuit occurs, in case of a pole-to-pole or pole-to-neutral fault. It takes a value of zero for pole-to-ground faults [p.u.].

For short-circuit simulations, this new equation is added to the matrix equation (7), introducing a new term, which results in equation (14):

$$\tau^C \frac{d[U]}{dt} = A[I^L] + B[I^C] + F[U] \tag{14}$$

Where:

F is a 5x5 matrix as shown in equation (15), where the fault conductance is introduced. For a particular case, all conductances are equal to zero, except for the ones with the name of the fault to be simulated. Fault names are summarized in Table I.

It should be noted that equation (12) remains unchanged for short-circuit simulations.

3. Software implementation of the model

The bipolar HVDC link with metallic return dynamic model has been implemented in a modular software framework developed by the authors in Matlab/Simulink [11]. This tool also includes a library of models for AC grids, Multi-Terminal HVDC grids, and different types of converters and generators. The software's modularity allows for the flexible integration of new models. It uses MatACDC to facilitate the initialization of the models after solving an AC/DC power flow [14]. These two aspects enable automatic flat start initialization and easy

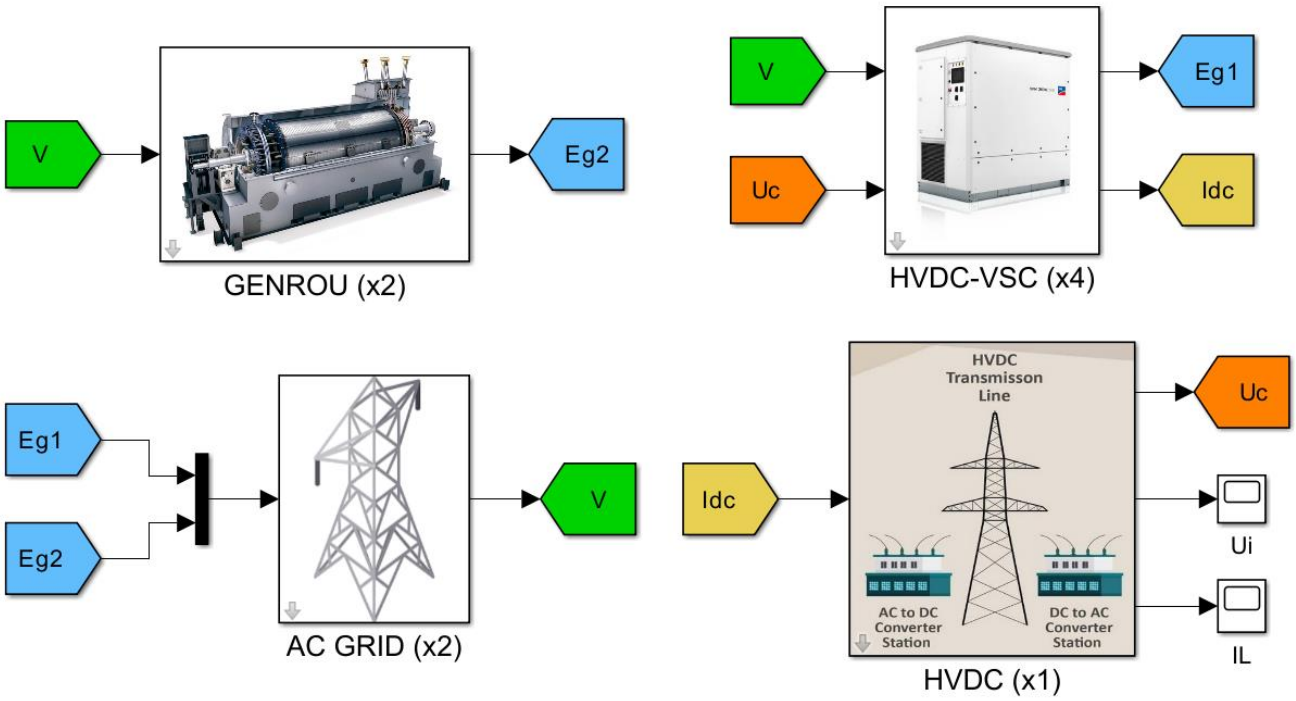

Fig. 2. Simulink interface in the software framework for the simulation results presented in this work.

$$F = \begin{bmatrix} -\mathrm{GA}^+ - \mathrm{GAA} & 0 & \mathrm{GAA} & 0 & 0 \\ 0 & -\mathrm{GB}^+ - \mathrm{GBB} - \mathrm{GBo}^+ & 0 & \mathrm{GBB} & \mathrm{GBo}^+ \\ \mathrm{GAA} & 0 & -\mathrm{GA}^- - \mathrm{GAA} & 0 & 0 \\ 0 & \mathrm{GBB} & 0 & -\mathrm{GB}^- - \mathrm{GBB} - \mathrm{GBo}^- & \mathrm{GBo}^- \\ 0 & \mathrm{GBo}^+ & 0 & \mathrm{GBo}^- & -\mathrm{GBo}^+ - \mathrm{GBo}^- \end{bmatrix} \tag{15}$$

configuration of new study cases. Fig. 2 shows the Simulink interface used to obtain the results presented in this paper. Four types of modules are used: conventional generators, converters, AC grids and the HVDC link model presented in this paper. The AC variables are the node voltages (V, in green), calculated by the AC grid model, and the internal voltage (Eg, in blue), is the output of the generator and converter models. The DC variables are the voltages at the converter terminals (Uc, in orange), calculated by the HVDC link model presented in this paper, and the converter current (Idc, in yellow), is the output of the converter model.

4. Results and discussion

This section presents the results of the simulations performed with the proposed bipolar HVDC link model with metallic return. The results analyze voltages and currents in the HVDC system under the three main types of faults that can be simulated: pole-to-ground, pole-to-neutral and pole-to-pole.

A. Pole-to-ground fault

This subsection presents the simulation results of a fault type A+ according to Table I, which is a pole-to-ground fault in the positive pole at the A-end of the line. The fault resistance is R = 0.1 Ω.

Fig. 3 presents the node voltages obtained from the simulation results. The results illustrate that the voltage in the positive pole falls close to zero when the fault takes place and recuperates after it is cleared. The negative pole is indirectly affected and suffers minor oscillations. The neutral acquires negative voltages during the contingency.

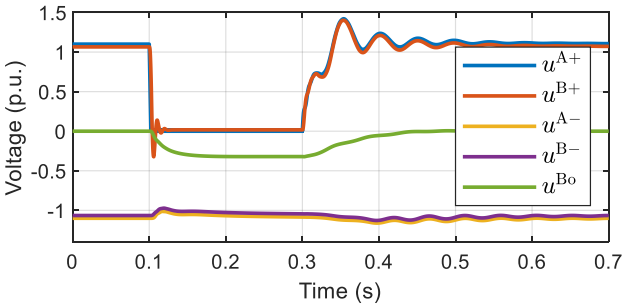

Fig. 3. Node voltages in a fault type A+ with R = 0.1 Ω

The currents flowing through the DC lines are presented in Fig. 4, where it can be observed that the current in the positive pole reaches negative values, close to zero, after a negative peak.

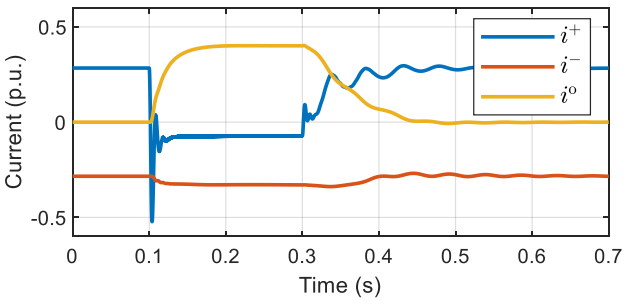

Fig. 4. Line currents in a fault type A+ with R = 0.1 Ω

Fig. 5 presents the converter currents. Converters CA+ and CB+ suffer a strong perturbation and their current output changes to maintain voltage. Converters CA- and CB- react to the contingency increasing the value of the current. This is due to the control mode they operate in, constant power, which increases the current to their limit when the voltage falls to maintain the power flow.

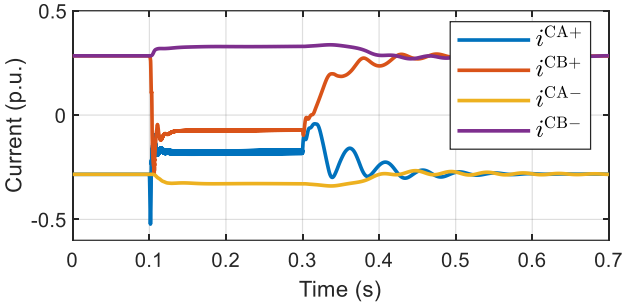

Fig. 5. Converter currents in a fault type A+ with R = 0.1 Ω

B. Pole-to-neutral fault

This subsection presents the simulation results of a fault type Bo+ according to Table I, which is a pole-to-neutral fault in the positive pole. The fault resistance is the same as in the previous case R = 0.1 Ω.

Fig. 6 shows the voltages in the nodes obtained from the simulation results. The voltage in the positive pole intersects at a midpoint with the neutral voltage, then both voltages become slightly negative. Oscillations are significant at node A+.

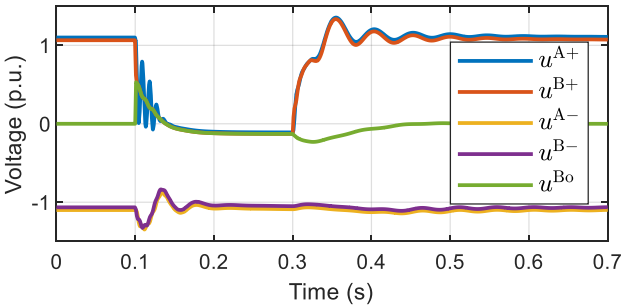

Fig. 6. Node voltages in a fault type Bo+ with R = 0.1 Ω

Fig. 7 presents the line currents in the HVDC cables. A transient with similar oscillatory behavior can be seen in the current of the positive pole. In the neutral cable, the current reaches -0.6 p.u. at the start of the fault, doubling the current that was previously running through the line.

C. Pole-to-pole fault

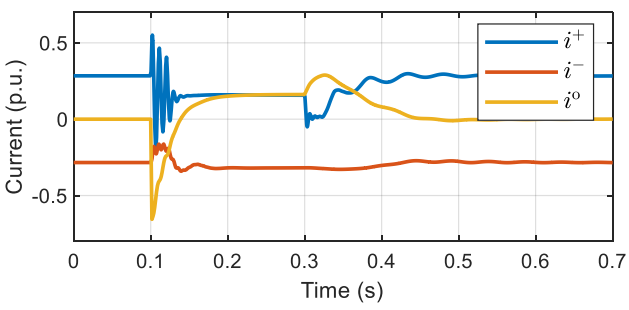

Fig. 7. Line currents in a fault type Bo+ with R = 0.1 Ω

This subsection presents the simulation results of a fault type AA, pole-to-pole, as shown in Table I. The fault resistance is R = 0.1 Ω as in the previous cases.

Fig. 8 shows the node voltages. A voltage dip occurs in both poles, that behave in a very similar way. The voltage in the neutral remains close to zero as this is a symmetric fault.

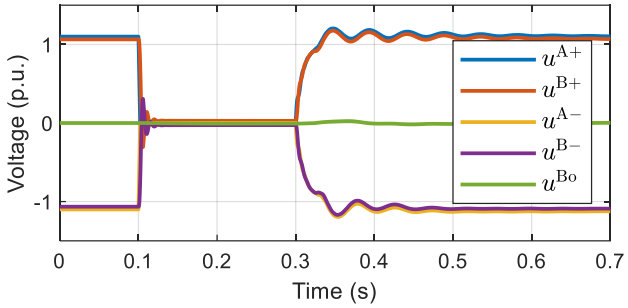

Fig. 8. Node voltages in a fault type AA with R = 0.1 Ω

Fig. 9 presents the line currents in the HVDC cables for the simulated contingency. The currents in both lines reverse direction when the short-circuit takes place, with all current supplying the fault. Once the fault is cleared, the currents recover their original values.

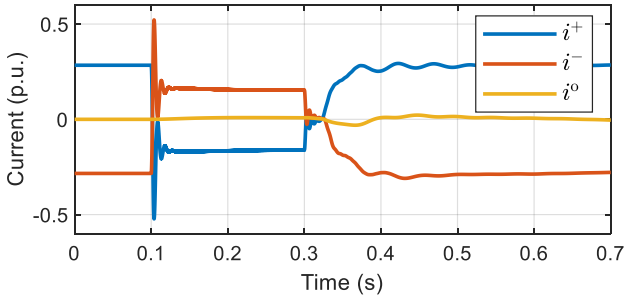

Fig. 9. Line currents in a fault type AA with R = 0.1 Ω

The results in this section have been provided to illustrate the versatility of the model, its capability to simulate different types of faults and to consider asymmetric behavior. They demonstrate the interaction between poles and the relevance of the neutral when asymmetric contingencies occur.

5. Conclusion

This work presents a dynamic model for bipolar HVDC links with metallic return. The model is flexible for simulating different types of faults and is formulated by only two dynamic matrix equations, which can be easily implemented in simulation software. The model has been integrated into a new module within a dynamic simulation tool in Matlab/Simulink with other models, incorporating automatic flat-start initialization. Altogether, this facilitates the easy preparation and configuration of different study cases. The model was tested with various fault types, demonstrating its functionality and the relevance of the neutral cable for asymmetric contingency simulations.

Acknowledgement

This work was supported by:

Spanish Research Agency under grant TED2021-130468B-I00 MCIN/AEI/MCIN/AEI/10.13039/501100011033 and by the European Union Next Generation EU/PRTR: Contribution of Grid ForMing converters to power systems stability and operability with high penetration of Renewable Energy Sources (GFM-RES).

Spanish Research Agency under grant PDC2022-133349-I00 funded by MCIN/AEI/10.13039/501100011033 and by the European Union "NextGenerationEU/PRTR": Prueba de concepto de convertidores formadores de red para contribuir al servicio de reposición del sistema eléctrico.

Comunidad de Madrid en el marco del convenio plurianual con la Universidad Carlos III Madrid en su línea de actuación "Excelencia para el Profesorado Universitario". V Plan Regional de Investigación Científica e Innovación Tecnológica 2016-2020.

References

[1] E. Pierri, O. Binder, N. Hemdan, and M. Kurrat, "Challenges and opportunities for a European HVDC grid," *Renewable and Sustainable Energy Reviews*, pp. 427–456, 2017, doi: 10.1016/j.rser.2016.11.233.

[2] A. Stan, S. Costinaș, and G. Ion, "Overview and Assessment of HVDC Current Applications and Future Trends," *Energies 2022, Vol. 15, Page 1193*, vol. 15, no. 3, p. 1193, Feb. 2022, doi: 10.3390/EN15031193.

[3] A. Alassi, S. Bañales, O. Ellabban, G. Adam, and C. MacIver, "HVDC Transmission: Technology Review, Market Trends and Future Outlook," *Renewable and Sustainable Energy Reviews*, vol. 112, pp. 530–554, Sep. 2019, doi: 10.1016/J.RSER.2019.04.062.

[4] N. R. Watson and J. D. Watson, "An Overview of HVDC Technology," *Energies (Basel)*, vol. 13, no. 4342, 2020, doi: 10.3390/en13174342.

[5] "Interconexión eléctrica por el Golfo de Bizkaia | Inelfe." Accessed: Jan. 22, 2025. [Online]. Available: https://www.inelfe.eu/es/proyectos/golfo-de-bizkaia

[6] "Offshore Network Development Plans European offshore network transmission infrastructure needs." Accessed: Jan. 29, 2024. [Online]. Available: https://www.entsoe.eu/outlooks/offshore-hub/tyndp-ondp/

[7] O. E. Oni, I. E. Davidson, and K. N. I. Mbangula, "A review of LCC-HVDC and VSC-HVDC technologies and applications," *EEEIC 2016 - International Conference on Environment and Electrical Engineering*, Aug. 2016, doi: 10.1109/EEEIC.2016.7555677.

[8] T. Kristian Vrana, J. Beerten, R. Belmans, and O. Bjarte Fosso, "A classification of DC node voltage control methods for HVDC grids," *Electric Power Systems Research*, vol. 103, pp. 137–144, 2013, doi: 10.1016/j.epsr.2013.05.001.

[9] R. B. Sinha, "UHVDC transmission with dedicated metallic return," *Proceedings of IEEE International Conference on Technological Advancements in Power and Energy, TAP Energy 2015*, pp. 485–488, Aug. 2015, doi: 10.1109/TAPENERGY.2015.7229667.

[10] P. Yang *et al.*, "Analysis on fault characteristic of metallic return in true bipolar VSC-HVDC transmission system," *IET Conference Publications*, vol. 2019, no. CP764, 2019, doi: 10.1049/CP.2019.0564.

[11] C. Wijnakker, F. Arredondo, J. L. Rodríguez-Amenedo, S. Delgado-Sánchez, and S. Arnaltes, "Generalized dynamic transient model for MTDC networks covering multiple topologies and contingencies," *Electric Power Systems Research*, vol. 243, p. 111469, Jun. 2025, doi: 10.1016/J.EPSR.2025.111469.

[12] C. Yang *et al.*, "Fault protection of multiterminal HVDC networks: Impact of inductance," *International Journal of Electrical Power & Energy Systems*, vol. 141, p. 108113, Oct. 2022, doi: 10.1016/J.IJEPES.2022.108113.

[13] "Type 4 - Generic Wind Turbine Generator Model (Phase II) - ESIG." Accessed: Feb. 03, 2025. [Online]. Available: https://www.esig.energy/wiki-main-page/type-4-generic-wind-turbine-generator-model-phase-ii/#Plant_level_control_model_.28repc_a.29

[14] J. Beerten and R. Belmans, "Development of an open source power flow software for high voltage direct current grids and hybrid AC/DC systems: MATACDC," *The Institution of Engineering and Technology*, vol. 9, no. 10, pp. 966–974, 2015, doi: 10.1049/iet-gtd.2014.0545.